INSTITUTE OF PHYSICS PUBLISHING JOURNAL OF PHYSICS: CONDENSED MATTER

J. Phys.: Condens. Matter **17** (2005) 257–267 doi:10.1088/0953-8984/17/2/002

Localization of 5f electrons and phase transitions in americium

M Pénicaud

Commissariat à l'Energie Atomique, DAM-Île de France, Département de Physique Théorique et Appliquée, BP 12, 91680 Bruyères-le-Châtel, France

E-mail: michel.penicaud@cea.fr

Received 20 September 2004, in final form 9 November 2004
Published 20 December 2004
Online at stacks.iop.org/JPhysCM/17/257

Abstract

Density-functional electronic calculations have been used to investigate the high-pressure behaviour of americium. The phase transitions calculated agree with the recent sequence obtained experimentally under pressure: double hexagonal close packed ($P6_3/mmc$) $\rightarrow$ face-centred cubic ($Fm\bar{3}m$) $\rightarrow$ face-centred orthorhombic ($Fddd$) $\rightarrow$ primitive orthorhombic ($Pnma$). In the first three phases the 5f electrons are found localized; only in the fourth phase (Am IV) are the 5f electrons found delocalized. The localization of the 5f electrons is modelled by an anti-ferromagnetic configuration which has a lower energy than the ferromagnetic ones. In this study the complex crystal structures have been fully relaxed.

(Some figures in this article are in colour only in the electronic version)

1. Introduction

Americium belongs to the series of actinide metals. It is known that the series of actinide metals, corresponding to the progressive filling up of the 5f electronic sub-shell, must be split in two. In the first sub-series, from Pa to Pu, the 5f electrons bind in the manner of d electrons in transition metals. In the other sub-series, starting with Am, the 5f electrons are localized, similarly to electrons in deep atomic layers, and like the 4f electrons of lanthanides they do not take part in metallic bonding. Another key distinction between the itinerant and localized regimes could be attributed to the possible formation of magnetic moments on the f-electron sites. Generally, the localized phase of an f-electron metal shows magnetic ordering at low temperatures according to Russell–Saunders coupling for a free ion; however, for Am, the f^6 ($J = 0$) ion configuration cancels the magnetic moment.

The localization of the 5f electrons is due to strong correlations between them that are not accurately treated by density functional calculations (DFT) with a local density approximation (LDA), and many attempts have been made to solve this problem. In the case of Am the localization of the 5f electrons at atmospheric pressure was simulated successively by a

ferromagnetic (FM) configuration [1, 2], by putting the 5f electrons in the atomic core [3], by decoupling them from the other band electrons [4, 5], by the self-interaction corrected (SIC) LDA [6, 7], and by a disordered local moment picture [8] within the LDA and the coherent potential approximation.

With the methods used in [3–5], of constrained LDA type, it is not possible to determine *ab initio* localized–delocalized transitions because the total energies calculated in constrained LDA and LDA are not comparable. In [1–8], except in [3], the calculations were simplified by the use of a face-centred cubic (fcc) structure instead of the double hexagonal close packed (dhcp) structure of ambient conditions. Moreover, in [1] and [8] the spin–orbit coupling was neglected, which is a rough approximation for a highly relativistic metal such as Am.

The previous element to Am, Pu, is believed [9] to have 5f electrons delocalized in its low-temperature α phase but localized to varying degree in the five higher-temperature phases (β, γ, δ, δ', ε). Recently special attention have been made to model the fcc δ structure due to the failure of the standard LDA or the improved generalized gradient approximation (GGA) which severely underestimate the equilibrium volume by up to 30% and, in addition, overestimate the bulk modulus about four times. δ-Pu is non-magnetic (NM) but good agreements with the experiment were obtained with an FM or an anti-ferromagnetic (AFM) configuration [10, 11], and the last one was found to have the minimum energy and to give the best results.

Independently of the real physical meaning of magnetism in δ-Pu, which is as yet an open question, this is a way to model the localization of the 5f electrons because it gives rise to a band splitting which reduces the bonding, resulting in an increased lattice constant and reduced bulk modulus. In the same way, Am is NM because of the cancellation between the spin and the orbital moments, which cannot be reproduced theoretically [2], but allowing magnetism in the theory permits a band splitting to simulate the localization of the 5f electrons. Generally speaking, the LDA fails to give the correct orbital moment when the orbital contribution to the magnetism is important, as in magnetic actinides, since the approximate treatment of exchange is not orbital dependent; even with the so-called 'orbital polarization' correction this cannot be rectified [2].

The next elements in the periodic table (Cm and Bk) have an AFM configuration [12], and they have the same dhcp structure as Am at ambient conditions; we plan to study them later on. The only reported magnetic measurements on Cf metal are in its metastable fcc phase and not in its dhcp equilibrium phase [12].

Allowing for magnetic configurations, FM or AFM but not non-collinear spins arrangements, we try in this study to reproduce the recent phase transitions found experimentally under pressure for Am [13].

2. Calculation details

All calculations were done using the all-electrons full potential linearized augmented plane wave (FPLAPW) program WIEN2k [14] in the GGA [15]. This code is fully relativistic for the core states and semi-relativistic with variational treatment of spin–orbit for the valence band. To make a significant comparison between different crystal structures to determine which is the most stable, the various parameters of the FPLAPW method, such as the choices of the muffin-tin radii ($R_{\mathrm{mt}} = 2$ bohr) and the truncations of basis and other expansions, are kept constant with the change of crystal structure. We used a large plane wave cut-off given by $R_{\mathrm{mt}} K_{\max} = 10$.

Local orbitals were added to enhance the variational freedom and allow the semi-core states 6s and 6p to be treated along with the valence electrons 7s, 7p, 6d and 5f. The new 'APW + lo (local orbital)' method [14, 16], which has some differences in the basis functions with the

standard LAPW method, is used for the 6d and 5f states because it converges more rapidly with the number of plane waves. Finally we extend the basis set of the second variational step by including $p_{1/2}$ local orbitals for a better description of the 6p states [14, 17] and we take a second-variation cut-off energy of 7 Ryd to ensure convergence.

During the self-consistent cycle, the integration over the irreducible part of the Brillouin zone is done using 'special-point' sampling [18]. For complex crystal structures, the more atoms a crystal cell contains, the fewer points are necessary for the integration over the whole Brillouin zone, which is smaller. We verify that the number of points in the whole Brillouin zone multiplied by the number of atoms in the unit cell (uc) gives about 1000 points in all the structures we consider.

In a recent paper [5] we reported studies of the structural stability of Am by comparison of the total energies calculated in 11 crystal structures. At high pressures the monoclinic α-Pu structure followed by the orthorhombic (space group $Pnma$) Am IV structure was found stable but not the face-centred orthorhombic (space group $Fddd$) Am III. Now we allow the magnetic configurations, which was not done previously, and we relax the structures, but we only consider the four structures found experimentally, dhcp Am I, fcc Am II, orthorhombic Am III and Am IV [13], and in addition the α-Pu structure [19].

In the dhcp structure [19] there are four atoms per unit cell (uc), two in positions 2a (0 0 0; 0 0 $\frac{1}{2}$) and two in positions 2d ($\frac{1}{3}$ $\frac{2}{3}$ $\frac{3}{4}$; $\frac{2}{3}$ $\frac{1}{3}$ $\frac{1}{4}$) of the space group $P6_3/mmc$. We choose the direction of magnetization along [001], the c-axis. We obtain a quasi-AFM configuration by putting the spin-up atoms in sites 2a and the spin-down atoms in sites 2d.

For the fcc structure, if we put the magnetization along [001] we create a tetragonal symmetry, body-centred ($I4/mmm$) in the FM case and primitive ($P4/mmm$) with 2 atoms/uc in the AFM case. These two atoms are in positions 1a (0 0 0) and 1d ($\frac{1}{2}$ $\frac{1}{2}$ $\frac{1}{2}$) [10]. If we put the magnetization along [111] we create a rhombohedral symmetry ($R\bar{3}m$) with 2 atoms/uc in the AFM case and only one atom in half of the previous unit cell in the FM case. Test calculations in the range where AFM fcc is stable, roughly from 180 to 140 bohr^3, revealed that the tetragonal symmetry had approximately from 1 to 5 mRyd/atom lower energy than the rhombohedral symmetry, and in the following we therefore only focus on the tetragonal symmetry.

In the orthorhombic Am III structure, the same as the γ-Pu structure, we put the magnetization axis along the longer dimension of the cell. For this structure many AFM configurations are possible: eight have been tested and after relaxation of the cell the most stable found reduces the symmetry to space group $F222$, which has 2 atoms/uc, with the spin-up atom in position 4a (0 0 0) and the spin-down atom in position 4c ($\frac{1}{4}$ $\frac{1}{4}$ $\frac{1}{4}$).

In the orthorhombic Am IV structure, a derivative of the α-U structure, there are 4 atoms/uc on 4c sites (x $\frac{1}{4}$ z; $\frac{1}{2}-x$ $\frac{3}{4}$ $z+\frac{1}{2}$; $-x$ $\frac{3}{4}$ $-z$; $x+\frac{1}{2}$ $\frac{1}{4}$ $\frac{1}{2}-z$) of $Pnma$. We put the spin-up atoms at $y = 1/4$ and the spin-down atoms at $y = 3/4$ with the magnetization along [010] to create an AFM configuration. The symmetry is reduced to space group $Pmc2_1$ with the spin-up atoms on 2a sites (0 y z; 0 $-$ y $z+\frac{1}{2}$) and the spin-down atoms on 2b sites ($\frac{1}{2}$ y z; $\frac{1}{2}-y$ $z+\frac{1}{2}$) of this space group.

In all cases the AFM configurations are alternate FM layers of spin-up or spin-down atoms with the magnetization axis orthogonal to the layers.

Unfortunately, there are many alternatives to order the spins in anti-parallel ways, especially for the more complex structures. Instead of our choice, the magnetization axis can be chosen parallel to the FM layers of atoms, or we can have AFM inside the layers. It is out of reach with the FPLAPW all-electron technique to examine all possibilities, because it would be too computer-time consuming; however, many configurations have been tested and the selected ones are the most stable.

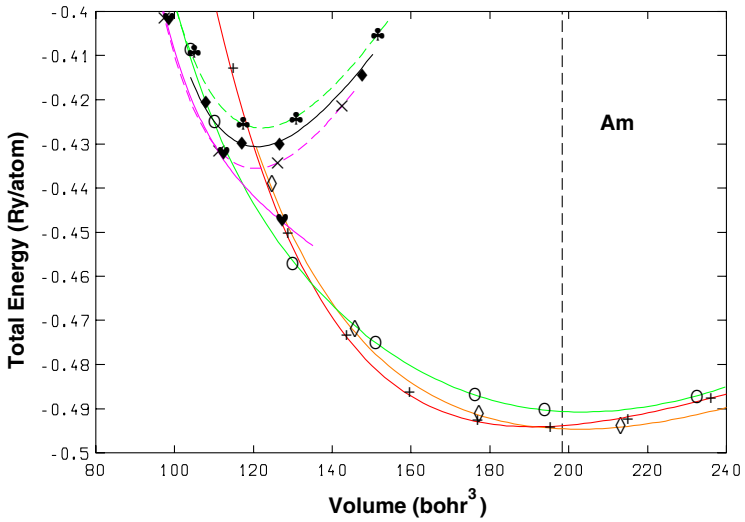

Figure 1. Total energies as functions of volume for Am, calculated in different crystal structures; dhcp (◊), fcc (+), Am III (○) and Am IV (♥) with an AFM configuration and Am III (♣), Am IV (×) and α-Pu (♦) assuming spin degeneracy. The room-temperature equilibrium volume for Am is denoted by a vertical broken curve.

3. Structural stability under pressure

In figure 1 we compare over a wide volume range the total energies of the considered crystal structures; this give us successively the most stable. The phase transitions now found theoretically agree with the recent sequence obtained experimentally under pressure [13]:

dhcp (Am I) → fcc (Am II) → face-centred orthorhombic (Am III) → primitive orthorhombic (Am IV).

In the first three phases the configuration is AFM, which is the one with the lowest energy; only in the fourth phase (Am IV) is the configuration NM. The AFM configuration is a way to treat the localized 5f electrons. When the first three phases theoretically exist, they are in this configuration, i.e. with localized 5f electrons, but when the Am IV phase appears at a theoretical pressure of 198 kbar and a theoretical volume of about 111 bohr^3, the magnetic moments of the AFM configuration have collapsed to nearly zero, which signals a complete 5f delocalization.

In this study the complex crystal structures have been fully relaxed except for the monoclinic α-Pu structure (16 atoms/uc) [19] for which it is a formidable task that involves two axial ratios, a unit cell angle and two internal parameters for eight atoms. Only the external parameters of the α-Pu structure have been optimized and the relaxation effects are found to be small, as has previously been said [20]. For an atomic volume of 125.5 bohr^3 the difference per atom is 1.34 mRyd between non-relaxed and relaxed results. At this volume the additional optimization of the two internal parameters of one atom lower the energy by only 0.1 mRyd. So the α-Pu structure is no longer found theoretically stable, as in past studies [2, 5], when this was inconsistent with the experiment [13].

In figure 2 can be seen the relatively small effects on the total energy of the relaxation of the α-Pu structure compared with the effects of the relaxations of the Am IV and particularly Am III structures. For the non-relaxed structures the internal crystallographic parameters and the axial ratios c/a, b/a are kept constant; for the α-Pu structure we use the values of Pu at

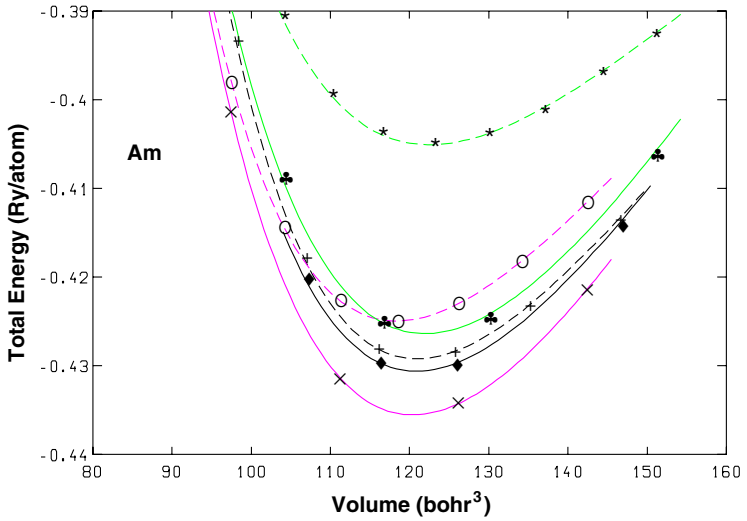

Figure 2. Comparison of total energies as functions of volume for Am, calculated with spin degeneracy, for relaxed Am III (♣), Am IV (×) and α-Pu (♦) crystal structures and for fixed to experimental parameters Am III (∗), Am IV (○) and α-Pu (+) crystal structures.

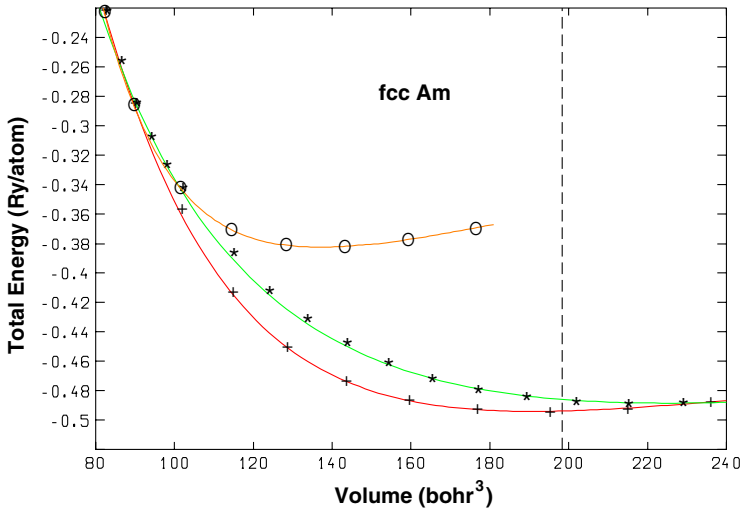

Figure 3. Total energies as functions of volume for Am, calculated in the fcc crystal structure assuming NM (○), FM (∗) and AFM (+) configurations with magnetization along [001], which creates a tetragonal symmetry. The room-temperature equilibrium volume for Am is denoted by a vertical broken curve.

ambient conditions [19], for the Am III structure the values of Am at 109 kbar [13], and for the Am IV structure the values at 890 kbar [13].

In figure 3 we compare in the fcc crystal structure the total energies for the NM, and with the magnetization along [001], the FM and AFM configurations; this last one has the lowest energy from the equilibrium volume to the volume of 89.5 bohr^3 where the magnetic moments collapse. According to figure 1, in all the range where it is stable, the fcc phase (Am II) is AFM, which means that it has localized 5f electrons.

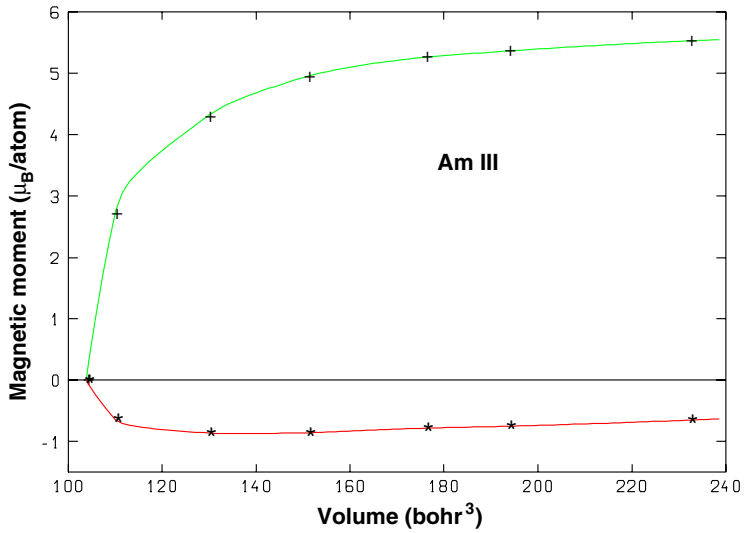

Figure 4. Spin (+) and orbital (∗) magnetic moments as functions of atomic volume for Am, calculated in the orthorhombic Am III structure in an AFM configuration.

What we have shown for fcc (Am II) can be shown for dhcp (Am I), the γ-Pu structure (Am III) or the orthorhombic Am IV, i.e. the AFM configuration has the lowest energy until the magnetic moments collapse at small volumes. From figure 1 we see that the Am I, Am II and Am III structures are AFM when they are stable; in contrast, the Am IV structure is NM because Am IV theoretically exists in the range of the small volumes.

In figure 4 we present the spin and orbital magnetic moments as a function of atomic volume for AFM Am in the γ-Pu structure (Am III). The spin moment slowly decreases in magnitude with volume, whereas the orbital moment is almost constant until about 110 bohr^3, where both moments collapse to zero, which can be interpreted as a signature of the delocalization of the 5f electrons in this crystal structure. The same phenomena happen in the other examined structures (dhcp, fcc, Am IV) which are AFM at large volumes until the magnetic moments disappear at small volumes; then the 5f electrons become itinerant and contribute to the chemical bonding between atoms.

Unfortunately, like in figure 4, in all the examined structures, at a given volume the spin moment is always greater than the orbital moment before they both collapse. The theory cannot reproduce here, like in [2], the cancellation between the spin and the orbital moments which is believed and which explains that Am is experimentally found to be NM [12].

In figure 5 we compare our theoretical isotherms with the experiment [13]. Our theoretical equilibrium volume, 200.4 bohr^3, in the dhcp structure is close to the experimental values, 198.4 bohr^3 [19] or 197.4 bohr^3 [13]. Our calculated bulk modulus is 256 kbar, also not too far from 297 kbar experimentally found [13]. These sufficiently good results explain that in figure 5 the experimental points are on the dhcp and fcc isotherms until 100 kbar; after this pressure they are on the Am III isotherm until 1 Mbar. Unfortunately at the experimental transition pressure of 160 kbar between Am III and Am IV, the Am IV isotherm is too far from the experimental values, the agreement is not obtained before 600 kbar where the Am III and Am IV isotherms meet.

In table 1 we report our calculated parameters of the phase transitions. From this table and figure 5 we see that we have a qualitative agreement with the experiment. We have improved

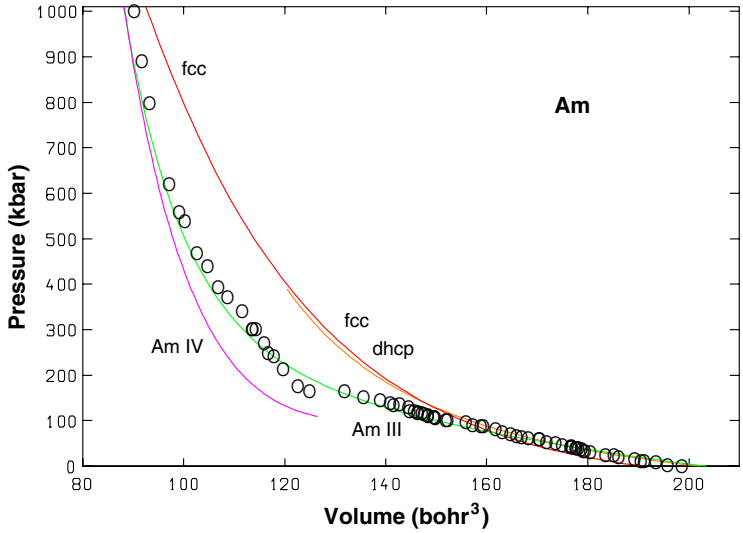

Figure 5. Pressures as functions of atomic volume for Am, calculated in the dhcp, fcc, Am III and Am IV crystal structures, which are the structures experimentally found. (O): experimental values [13].

Table 1. Comparison of our calculated (cal) and the experimental (exp) [13] pressures (P) and volume variations ($\Delta V/V$) at the phase transitions.

Phase transitions	P_{cal} (kbar)	P_{exp} (kbar)	$\Delta V/V_{\mathrm{cal}}$ (%)	$\Delta V/V_{\mathrm{exp}}$ (%)
dhpc → fcc	7	61	5	0
fcc → Am III	186	100	10	2
Am III → Am IV	198	160	10	7

the results of the previous theoretical studies, especially for the pressure of the localization–delocalization transition of the 5f electrons (ldt_5f) which happens with the crystalline change Am III → Am IV. In [2] for ldt_5f, 80 kbar was obtained for a transition from the FM fcc structure to the NM α-Pu structure. In [7] for ldt_5f, 430 kbar was obtained by the SIC-LDA method, in a calculation restricted to the fcc structure by means of delocalizing one 5f electron.

In the previous theoretical studies of the structural transitions in Am [2, 5] the crystal structures were not optimized, except for the orthorhombic α-U structure in [2]. Here all our examined structures are relaxed, and we see in figures 6–8 that the axial ratios and internal parameters are far from constant with compression. In figures 6 and 7 our theoretical values for the Am III and Am IV structures are close to the given experimental ones [13]. In figure 8 we see some differences between the relaxed parameters of the monoclinic α-Pu structure in Am and the value of these parameters in α-Pu at its equilibrium volume, although the consequences on the total energies are small in figure 2.

At the equilibrium volume of Am in the dhcp structure we obtain 3.19 for the axial ratio c/a; the experimental value is 3.24 [13, 19], the 'ideal' value being 3.267.

4. Electronic structure

In figure 9 our calculated density of states (DOS) of Am at its equilibrium volume in the AFM dhcp structure shows two 5f peaks and the Fermi energy (E_{F}) between them. There is, however, a small 5f contribution at E_{F}, which gives for the DOS at E_{F}; $D_{\mathrm{F}} = 2.2$ states/eV/atom.

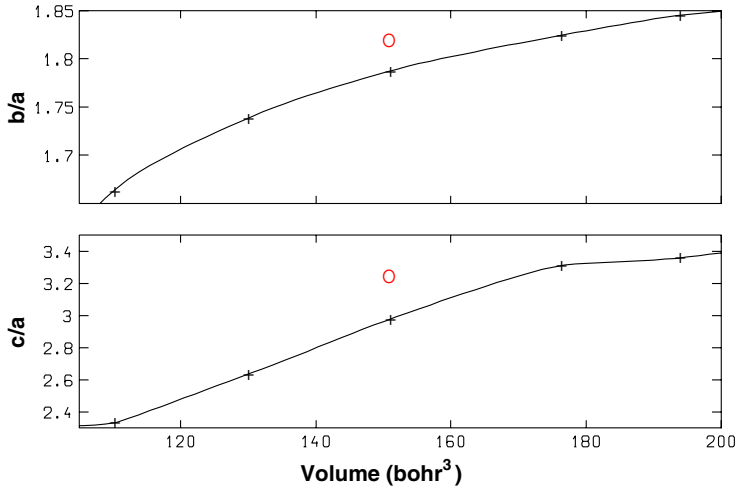

Figure 6. Calculated evolution of the parameters of the orthorhombic Am III structure with atomic volume. (O): experimental values [13].

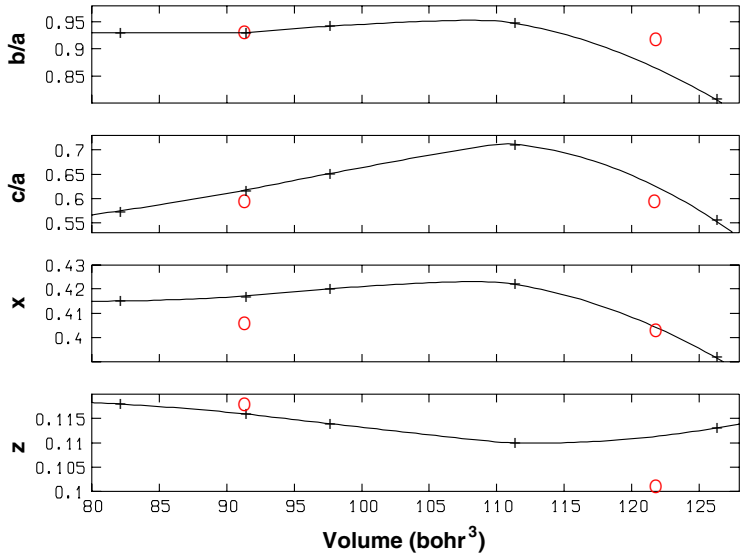

Figure 7. Calculated evolution of the parameters of the orthorhombic Am IV structure with atomic volume. (O): experimental values [13].

In a first approximation the electronic specific heat coefficient γ is proportional to D_F [21], which yields $\gamma_{th} = 5.3$ mJ mol^{-1} K^{-2}. There is some uncertainty on the experimental value of γ [12], but γ_{th} is a possible value and would not be in contradiction with a light rare-earth character for Am [12].

Our DOS of figure 9 can be compared with the DOS obtained for Am in the fcc structure with the fully relativistic muffin-tin orbital (MTO) method [4]. In this way, the first peak in figure 9 can be associated with the $5f_{5/2}$ sub-shell being almost full, i.e. a little less than six $5f_{5/2}$ electrons; the second peak is associated with the $5f_{7/2}$ sub-shell being almost empty.

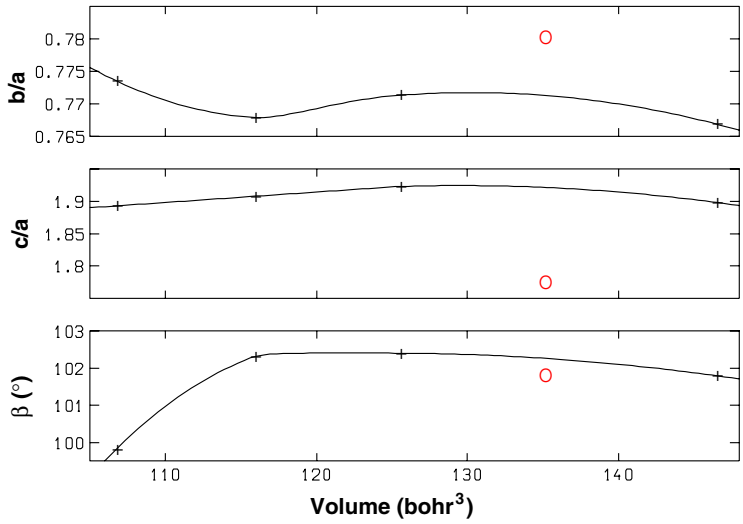

Figure 8. Calculated evolution of the parameters of the monoclinic α-Pu structure with atomic volume in Am. (O): experimental values of α-Pu at its equilibrium volume [19].

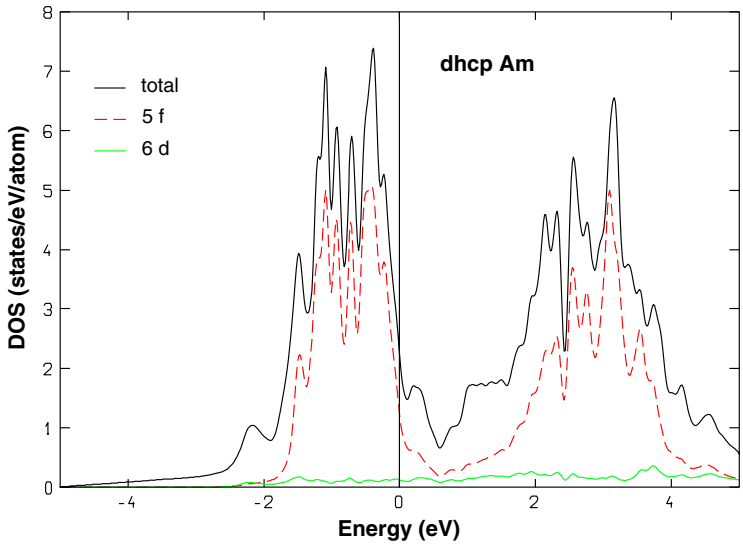

Figure 9. Densities of states for AFM dhcp Am at the equilibrium volume (198.4 bohr^3). The DOSs have been convoluted with a Gaussian function of width 0.05 eV. Energies are relative to the Fermi energy.

Our DOS can also be compared with the x-ray and ultra-violet photoemission spectra obtained for Am [22], which show the 5f states withdrawn from the Fermi level and forming a broad peak structure before E_F, of which the exact nature is still a matter of debate [23]. The $5f_{5/2}$ peak of our DOS is centred 1 eV before E_F instead of 2.8 eV experimentally found [22].

In contrast to Am, the photoemission results for α-Pu and δ-Pu present the strongest emissions, related to 5f electrons, just positioned at E_F [24, 25] and the δ-Pu emission, narrower than in α-Pu, is suggestive of a semi-localization of the 5f electrons. We have calculated the

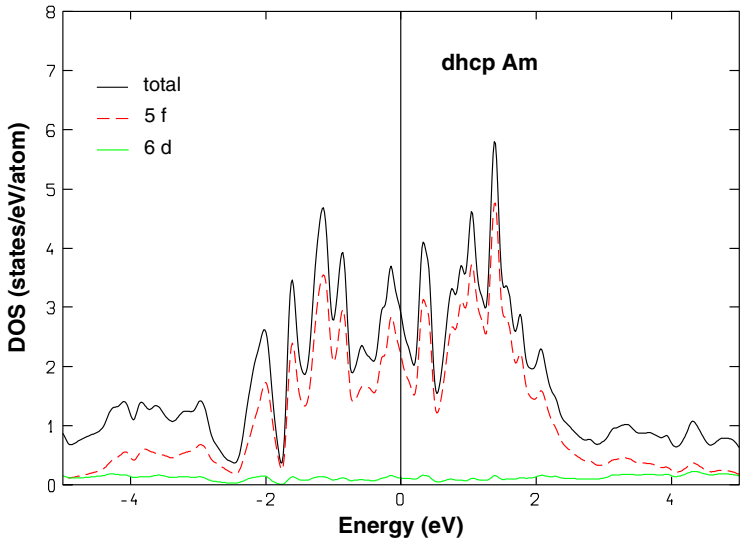

Figure 10. Densities of states for dhcp Am at a small volume (88.4 bohr^3) where the magnetic moments have collapsed. The DOSs have been convoluted with a Gaussian function of width 0.05 eV. Energies are relative to the Fermi energy.

DOS for α-Pu with FPLAPW [26] and obtained a broad peak at E_F due to itinerant 5f electrons. The DOSs for δ-Pu have been calculated with MTO [26] where the couplings between the $5f_{5/2}$ and the s, p, d electrons have been removed; this gives a very narrow $5f_{5/2}$ peak pinned at E_F and a proportional [21] very high γ value in agreement with the experiment [27].

In figure 10 we show the DOS for the dhcp structure at a small volume (88.4 bohr^3), where the magnetic moments have collapsed, for comparison with the DOS at the equilibrium volume (198.4 bohr^3), where the AFM configuration is stable. At ambient conditions we can see the two 5f peaks separated by a wide gap, the 5f electrons are localized in energy. For the small volume the peaks have disappeared; the 5f electrons are delocalized.

5. Conclusion

The phase transitions found theoretically by DFT calculations for Am agree at least qualitatively with the recent sequence obtained experimentally under pressure [13]:

dhcp (Am I) $\rightarrow$ fcc (Am II) $\rightarrow$ face-centred orthorhombic (Am III) $\rightarrow$ primitive orthorhombic (Am IV).

In the first three phases the 5f electrons are found to be localized, and this is modelled by an AFM configuration which has a lower energy than the FM or NM ones. The Am IV structure is found to be NM because in the high pressure range where it is stable the magnetic moments have collapsed, which can be interpreted as a delocalization of the 5f electrons.

We have also shown the large effect of the relaxation of the complex crystal structures on the total energy calculated at a given volume.

It is not fully satisfactory to have not obtained the cancellation of the spin moment by the orbital moment which is believed in Am [12] to explain why this metal is experimentally NM at ambient conditions. Of all attempts [1–8] to model Am at ambient conditions, only one [6] has almost succeed in doing that, with calculations in an FM fcc crystal structure, by adding to the usual LDA potential an ad hoc repulsive scalar potential $V_{f7/2}$ for the state

$5f_{7/2}$. The resulting electronic configuration was close to the NM $5f^6$ ($N_f = 6.03$) and the spin moment ($-2.97\ \mu_B$) almost compensated by the orbital moment ($2.865\ \mu_B$), but the $5f_{5/2}$ peak of the DOS is shifted 7 eV before E_F, too much for the 2.8 eV experimentally found [22]. This method is also of constrained LDA type and, as with the methods in [3–5], cannot treat a localization–delocalization transition.

In summary, allowing an AFM configuration has permitted us to model the behaviour of Am at ambient conditions and under pressure, and with an improved exchange–correlation functional it will be perhaps be possible to obtain the cancellation, generally believed, between the spin and the orbital moments.

References

[1] Skiver H L, Andersen O K and Johansson B 1978 *Phys. Rev. Lett.* **41** 42
[2] Söderlind P, Ahuja R, Eriksson O, Johansson B and Wills J M 2000 *Phys. Rev.* B **61** 8119
[3] Eriksson O, Brooks M S S and Johansson B 1990 *J. Less-Common Met.* **158** 207
[4] Pénicaud M 1997 *J. Phys.: Condens. Matter* **9** 6341
[5] Pénicaud M 2002 *J. Phys.: Condens. Matter* **14** 3575
[6] Solov'ev I V, Likhtenshtein A I and Gubanov V A 1991 *Sov. Phys.—Solid State* **33** 572
[7] Petit L, Svane A, Temmerman W M and Szotek Z 2000 *Solid State Commun.* **116** 379
[8] Niklasson A M N, Wills J M, Katsnelson M I, Abrikosov I A, Eriksson O and Johansson B 2003 *Phys. Rev.* B **67** 235105
[9] Wallace D C 1998 *Phys. Rev.* B **58** 15433
[10] Wang Y and Sun Y 2000 *J. Phys.: Condens. Matter* **12** L311
[11] Söderlind P 2001 *Europhys. Lett.* **55** 525
[12] Fournier J M and Troć R 1985 *Handbook on the Physics and Chemistry of the Actinides* vol 2, ed A J Freeman and G H Lander (Amsterdam: North-Holland) p 29
[13] Heathman S, Haire R G, Le Bihan T, Lindbaum A, Litfin K, Méresse Y and Libotte H 2000 *Phys. Rev. Lett.* **85** 2961
Lindbaum A, Heathman S, Litfin K, Méresse Y, Haire R G, Le Bihan T and Libotte H 2001 *Phys. Rev.* B **63** 214101
[14] Blaha P, Schwarz K, Madsen G K H, Kvasnicka D and Luitz J 2001 *WIEN2k* ed K Schwarz (Vienna: Vienna University of Technology)
[15] Perdew J P, Burke S and Ernzerhof M 1996 *Phys. Rev. Lett.* **77** 3865
[16] Sjöstedt E, Nordström L and Singh D J 2000 *Solid State Commun.* **114** 15
[17] Kuneš J, Novák P, Schmid R, Blaha P and Schwarz K 2001 *Phys. Rev.* B **64** 153102
[18] Chadi D J and Cohen M L 1973 *Phys. Rev.* B **8** 5747
[19] Wyckoff R W G 1963 *Crystal Structures* vol 1 (New York: Wiley)
[20] Söderlind P and Sadigh B 2004 *Phys. Rev. Lett.* **92** 185702
[21] Ziman J M 1972 *Principle of the Theory of Solids* (Cambridge: Cambridge University Press) p 144
[22] Naegele J R, Manes L, Spirlet J C and Müller W 1984 *Phys. Rev. Lett.* **52** 1834
[23] Mårtensson N, Johansson B and Naegele J R 1987 *Phys. Rev.* B **35** 1437
[24] Arko A J, Joyce J J, Morales L, Wills J, Lashley J, Wastin F and Rebizant J 2000 *Phys. Rev.* B **62** 1773
[25] Tobin J G, Chung B W, Schulze R K, Terry J, Farr J D, Shuh D K, Heinzelman K, Rotenberg E, Waddill G D and van der Laan G 2003 *Phys. Rev.* B **68** 155109
[26] Pénicaud M 2000 *J. Phys.: Condens. Matter* **12** 5819
[27] Lashley J C, Singleton J, Migliori A, Betts J B, Fisher R A, Smith J L and McQueeney R J 2003 *Phys. Rev. Lett.* **91** 205901